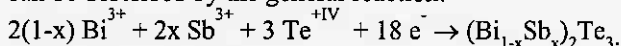


Electroplating and characterization of $(\text{Bi}_{1-x}\text{Sb}_x)_2\text{Te}_3$ thermoelectric films

D. Del Frari, S. Diliberto, N. Stein, C. Boulanger, J.M. Lecuire
Laboratoire d'Electrochimie des Matériaux – UMR CNRS 7555
Université de Metz, 1 Bd Arago, Technopôle, 57078 METZ Cedex 3, FRANCE
e-mail : delfrari@sciences.univ-metz.fr

Abstract

In this paper, the processes associated with the electrodeposition of bismuth antimony telluride thermoelectric films, were reported along with an analysis of the composition and crystallinity of the resulting films. The electrodeposition can be described by the general reaction:

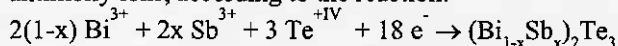


Cyclic voltammetry study led to the determination of the deposition potential of the ternary Bi-Sb-Te dissolved in 1M perchloric acid and 0,1M tartaric acid. The influence of the potential deposition and the electrolyte composition on film stoichiometry have been studied. It was shown that all stoichiometries of the $\text{Bi}_x\text{Sb}_{2-x}\text{Te}_3$ solid solution can be easily adjusted by controlling the potential deposition and the electrolyte solution. However, these films present an important roughness. The roughness decreases by synthesis films with a pulse technique. Seebeck coefficient and electrical resistivity are also improved with this technique.

Introduction

Thermoelectricity is the phenomenon which results from the direct conversion of heat into electrical energy (or vice versa) [1]. The thermoelectric efficiency is defined by the figure of merit Z , which can be expressed as a function of the Seebeck coefficient α , the electrical resistivity ρ , and the thermal conductivity λ , according to the relation $Z = \alpha^2 / \rho\lambda$. Good thermoelectric properties are achieved for a high Z -value, which is associated with a high α -value and low ρ - and λ -values. Bismuth-based semiconductors are commonly used for thermoelectric devices such as thermoelectric generators [2,3] and coolers [4] and for optical storage systems [5]. Bismuth telluride Bi_2Te_3 and its derivative compounds are considered to be the best materials for use in thermoelectric refrigeration at room temperature [6,7], in particular $\text{Bi}_2\text{Te}_{2.7}\text{Se}_{0.3}$ and $\text{Bi}_{0.5}\text{Sb}_{1.5}\text{Te}_3$ for the n-type and p-type, respectively. These materials are generally synthesised by directional crystallisation techniques [8-10], powder metallurgy process [11] or evaporation methods [12-15]. However, these techniques do not readily lend themselves to the production of large-area thermo-elements. Electrochemical deposition may provide an alternative process to these classical methods. Indeed, this technique has a relatively simple procedure and allows deposition of the thermoelectric films onto electrodes of variable geometry and obtaining specific materials necessary for solving the thermal management of electronic devices, for example. If the electrodeposition has been successfully applied to the production of bismuth telluride binaries [16-19] and Bi-Te-Se ternary [20], there are few studies concerning the Bi-Sb-Te ternary. That is why the aim of this work was to produce $\text{Bi}_x\text{Sb}_y\text{Te}_z$, and more particularly the $\text{Bi}_{0.5}\text{Sb}_{1.5}\text{Te}_3$ alloy. As the process of binary alloys deposition is based on the

electroreduction of tellurite ions in the presence of bismuth salts, we supposed that the bismuth ions can be substituted by antimony ions, according to the reaction:



The present work concerns in particular the definition of the optimum conditions for a potentiostatic plating and a pulse electrodeposition of Bi-Sb-Te. Finally, the composition, thickness and annealing temperature dependence of electrical and thermoelectric properties of Bi-Sb-Te films at room temperature have been analysed.

Experimental details

The reaction analysis was realized by voltamperometric techniques. Voltammetric experiments were carried out in a conventional three-electrode cell at room temperature. The electrolyte solution was deaerated by argon bubbling for 30 min prior to the experiment and this atmosphere was kept constant during this experiment. The working electrode was a non-rotating platinum disc (2 mm diameter), in order to keep a natural diffusion mode. The scan rate was fixed at 0,5 mV/s. The electrochemical potentials of the working electrode were measured and expressed by reference to a saturated calomel electrode (SCE). The counter electrode was a platinum disc (10 mm diameter). The experiments were realized without stirring. The linear sweep voltammograms were obtained using a Radiometer PGZ 301, Voltmaster 4 software and an IBM PC computer. The electrolyte baths were prepared with Millipore water (10 M Ω .cm) and analytical grade reagents. To ensure the stability and the solubility of bismuth(III), antimony(III) and tellurium(IV) species in solution, the selected solvent was a solution containing tartaric acid (0,1M) for its chelating properties in relation to antimony, and perchloric acid (1M) for its acid properties. The solutions were respectively obtained by dissolution of Bi_2O_3 , Sb_2O_3 and TeO_2 . The tellurite concentration was fixed at 10^{-2} M.

Stainless steel discs were chosen as substrate for potentiostatic deposition. Plates were mechanically polished with silicium paper and with diamond paste (1 μm size). After being polished, the electrodes were cleaned with distilled water followed by ethanol rinsing. The working electrodes were located horizontally in the bottom of a PTFE cell specially designed in our laboratory. A 2 cm² area was exposed for deposition. The cathodic polarization was carried out at room temperature without stirring and was realized with the same reference and counter electrodes as voltammetric study. The electrochemical cell, under an argon atmosphere, had an electrolyte volume of 0,1 dm³ and the concentrations were similar to these of the voltammetric study.

Samples were prepared after electrodeposition by thorough rinsing in three steps (nitric acid solution pH 1, Millipore water and ethanol) followed by drying in air. X-ray diffraction data were obtained with an Inel diffractometer (XRG 2500

CPS 120, CuK α radiation). The sample composition were obtained by electron probe microanalysis (CAMECA SX50 and SX100).

The electrical properties of the electrodeposited (Bi $_{1-x}$ Sb $_x$) $_2$ Te $_3$ materials were determined measuring the Seebeck coefficient and electrical resistivity. The Seebeck coefficient was measured using a Keithley 27000 multimeter. The temperatures and the differential potential of the film were measured using 0,1 mm diameter K type standard thermocouples. Electrical resistivity was measured using the four point technique, with a HEM-2000 EGK system. All annealings were realized in a Thermolyne 21100 tube furnace under primary vacuum.

Results and discussion

1. Potentiostatic deposition

✓ Influence of the deposition potential

A tartaric-perchloric electrolyte, with a cation to tellurium ratio equal to 1, allows the electroplating of Sb $_2$ Te $_3$ and Bi $_2$ Te $_3$ binaries [21]. The same cations to tellurium ratio was chosen for the ternary study, i-e ([Bi]+[Sb])/[Te]=1. Concerning the [Sb]/[Bi] ratio, the stoichiometry of the expected ternary Bi $_{0,5}$ Sb $_{1,5}$ Te $_3$ had governed our choice of a [Sb]/[Bi] ratio equal to 3.

The cathodic scan presents three reduction waves (Figure 1). The first level noted (c $_1$) is ranging between 150 and -50 mV/SCE and it would be representative of reduction of Te $^{IV+}$ in Te 0 , as well as the obtention of Bi $_2$ Te $_3$. The intermediate level (c $_2$), ranging between -50 and -150 mV/SCE, concerns the obtention of a Bi $_x$ Sb $_y$ Te $_z$ ternary from the X-Ray characterization. The third level (c $_3$), from -150 and -250 mV/SCE, is characteristic of the ternary Bi $_{0,5}$ Sb $_{1,5}$ Te $_3$ obtention.

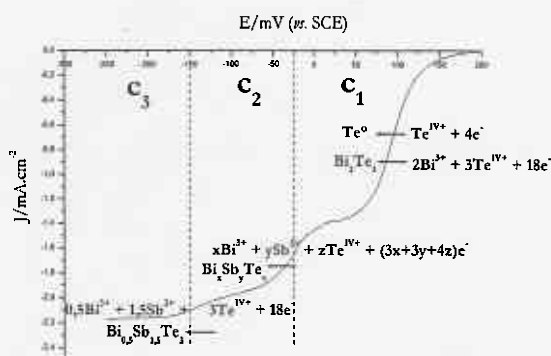


Fig.1 Voltamperogram in 1M HClO $_4$ -0,1M C $_4$ H $_6$ O $_6$ of a Bi-Sb-Te solution, ([Sb $^{III+}$]+[Bi $^{III+}$])/[Te $^{IV+}$]=1 and [Sb $^{III+}$]/[Bi $^{III+}$]=3, [Te $^{IV+}$]=10 $^{-2}$ M - Working electrode: Pt - Without stirring - Surface area: 3,14 mm 2 - Potential sweep rate: 0,5 mV/s

The alternative deposited materials obtained for these three waves of potentials were analysed by X-Ray diffraction (Figure 2). Concerning the (c $_3$) wave, the film obtained at -170 mV/SCE is crystallised and single phased. The X-Ray diffraction pattern presents the characteristic peak of Bi $_{0,5}$ Sb $_{1,5}$ Te $_3$ (11.0), and all diffraction lines could be indexed to the hexagonal rhombohedral structure of this ternary (ASTM 49-1713).

For cathodic potentials corresponding to the second level (c $_2$), a film was obtained at -100 mV/SCE. The pattern presents a Bi $_{0,5}$ Sb $_{1,5}$ Te $_3$ structure justified by its diffraction characteristic peak. In addition, a small shift of peaks is observed, probably due to an excess of bismuth. Furthermore, a specific peak of Te 0 is observed. The level ranging between 150 and -50 mV/SCE (c $_1$) was studied for a potential of -20 mV/SCE. The obtained pattern does not have the specific peak of the expected ternary, but presents a Bi $_2$ Te $_3$ structure, and also the characteristic peak of Te 0 .

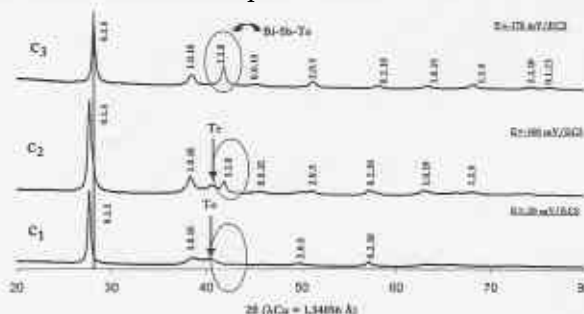


Fig.2 X-Ray diffraction diagram of Bi-Sb-Te electrodeposit obtained under potentiostatic conditions ([Bi $^{III+}$]+[Sb $^{III+}$]=[Te $^{IV+}$]=10 $^{-2}$ M, [Sb $^{III+}$]/[Bi $^{III+}$]=3)

The potential dependence of the alloy stoichiometry is presented in Figure 3. For potentials corresponding to the first level (c $_1$), the film compositions are near to BiTe $_4$, but the crystallographic study demonstrates the presence of two forms: Bi $_2$ Te $_3$ and Te 0 . These two structures can not be differentiated by electron probe microanalysis, but it can be easily calculated that the film is composed of 55% (weight %) of Bi $_2$ Te $_3$. Concerning the second level (c $_2$), the stoichiometry confirms the obtention of a Bi $_x$ Sb $_y$ Te $_z$ compound with an excess of tellurium corresponding to the presence of Te 0 evidenced by X-ray diffraction. The curves show that the ratio Bi $_x$ Sb $_y$ Te $_z$ /Te 0 depends strongly on potential. Finally, for the third level (c $_3$), the composition of Bi $_{0,5}$ Sb $_{1,5}$ Te $_3$ film does not depend on potential for -300 to -150 mV/SCE range. These results confirm the previous crystallographic and voltammetric studies.

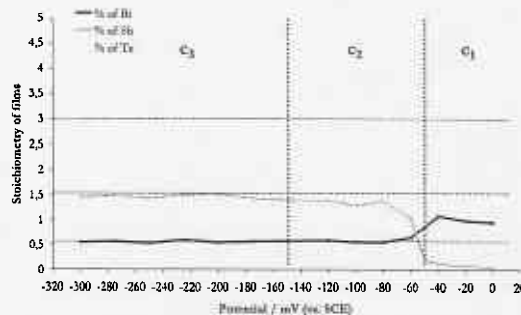


Fig.3 Potential dependence of Bi $_x$ Sb $_y$ Te $_z$ stoichiometry [Bi $^{III+}$]+[Sb $^{III+}$]=[Te $^{IV+}$]=10 $^{-2}$ M, [Sb $^{III+}$]/[Bi $^{III+}$]=3

The Seebeck coefficient and electrical resistivity measurements were performed on (Bi $_{1-x}$ Sb $_x$) $_2$ Te $_3$ materials in order to determine time and temperature of annealing corresponding to the highest properties. These measurements were performed on the Bi $_{0,5}$ Sb $_{1,5}$ Te $_3$ films, which are considered to present the best thermoelectric properties.

The annealing temperature dependence of the Seebeck coefficient is presented in Figure 4, for different annealing times. The α coefficient increases with increasing temperature from 150°C to 250°C, excepted for a time of 240 minutes, where two temperatures, 150°C and 250°C, presented the same results. The best value of thermoelectric power was obtained for a 60 minutes annealing at 250°C, and was about 170 μ V/K.

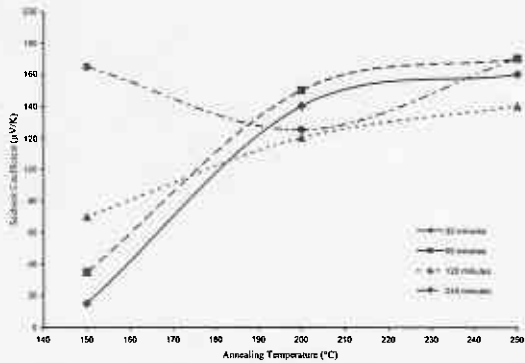


Fig.4 Evolution of the Seebeck coefficient α with the annealing temperature of $\text{Bi}_{0.5}\text{Sb}_{1.5}\text{Te}_3$ electroplated film ($E_{\text{deposition}} = -170$ mV/SCE, $[\text{Bi}^{\text{III}+}] + [\text{Sb}^{\text{III}+}] = [\text{Te}^{\text{IV}+}] = 10^{-2}\text{M}$, $[\text{Sb}]/[\text{Bi}] = 3$)

Figure 5 shows the plot of electrical resistivity vs. annealing temperature for a 6 μ m thickness film. ρ decreases with increasing temperature for 30 and 60 minutes annealing, and increases for a more long time of annealing. The best value of electrical resistivity was about 550 $\mu\Omega\cdot\text{m}$, and was obtained for conditions similar as the best value of α , i.e after a 60 minutes annealing at 250°C.

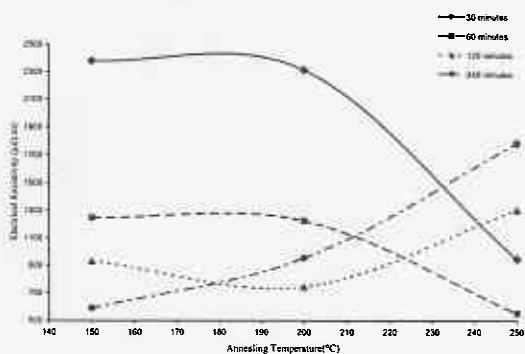


Fig.5 Evolution of the electrical resistivity ρ with the annealing temperature of $\text{Bi}_{0.5}\text{Sb}_{1.5}\text{Te}_3$ electroplated film ($E_{\text{deposition}} = -170$ mV/SCE, $[\text{Bi}^{\text{III}+}] + [\text{Sb}^{\text{III}+}] = [\text{Te}^{\text{IV}+}] = 10^{-2}\text{M}$, $[\text{Sb}]/[\text{Bi}] = 3$)

✓ Influence of $[\text{Sb}]/[\text{Bi}]$ ratio in solution

The Bi-Sb-Te ternary phase diagram at $T = 20^\circ\text{C}$ [22] indicates the existence of a solid solution between Bi_2Te_3 and Sb_2Te_3 . In order to obtain each possible stoichiometry between these two binaries, different $[\text{Sb}]/[\text{Bi}]$ ratios were studied ($[\text{Sb}]/[\text{Bi}] = 2, 3, 4$ and 6), with a constant $([\text{Bi}] + [\text{Sb}])/[\text{Te}]$ ratio equal to 1.

The cathodically deposited materials obtained for different ratios at -170 mV/SCE were analysed by X-Ray diffraction (Figure 6). Diffraction patterns evidence a better crystallinity

for the films with a low atomic antimony content obtained with a small $[\text{Sb}]/[\text{Bi}]$ ratio. Moreover, a small shift of peaks is observed when the bismuth percentage in solution increases.

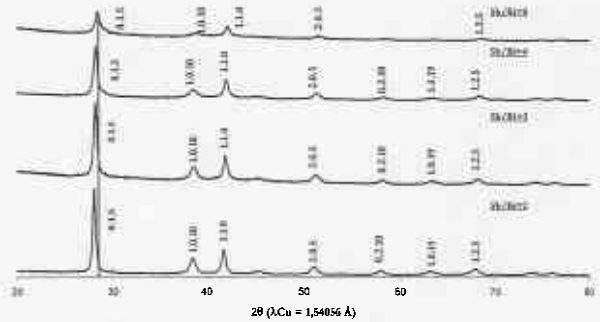


Fig.6 X-Ray diffraction diagram of Bi-Sb-Te electrodeposit obtained under potentiostatic conditions, for different $[\text{Sb}^{\text{III}+}]/[\text{Bi}^{\text{III}+}]$ ratios ($E_{\text{deposition}} = -170$ mV/SCE, $[\text{Bi}^{\text{III}+}] + [\text{Sb}^{\text{III}+}] = [\text{Te}^{\text{IV}+}] = 10^{-2}\text{M}$)

The evolution of the film composition with the $[\text{Sb}]/[\text{Bi}]$ ratio in solution is presented in Figure 7. All films have a $(\text{Bi}_x\text{Sb}_{1-x})_2\text{Te}_3$ structure, but the antimony and bismuth percentages in the film depend linearly on the $[\text{Sb}]/[\text{Bi}]$ ratio in solution. This curve evidences that an electrolyte with a bismuth atomic percentage of 11.6% allows to obtain a film having a bismuth atomic percentage of 10% corresponding to the composition of $\text{Bi}_{0.5}\text{Sb}_{1.5}\text{Te}_3$.

Therefore, it is possible to obtain each stoichiometry of materials according to the initial $[\text{Sb}]/[\text{Bi}]$ ratio in solution.

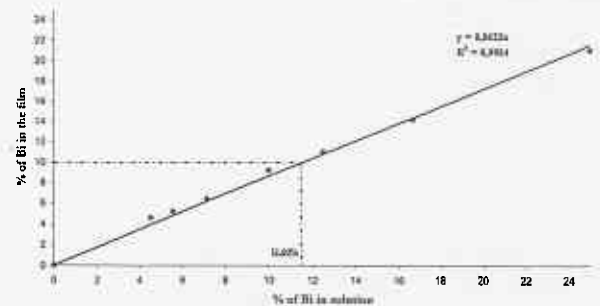


Fig.7 Relation between the Bi atomic percentage in film with the Bi atomic percentage in solution -- $E = -170$ mV/SCE

The evolutions of the Seebeck coefficient and electrical resistivity with the bismuth atomic percentage in the film were studied in order to determine the type of the $(\text{Bi}_{1-x}\text{Sb}_x)_2\text{Te}_3$ semi-conductors, and the composition corresponding to the best properties before and after annealing.

The evolution of the Seebeck coefficient α with the composition is reported in Figure 8. It appears that the $(\text{Bi}_{1-x}\text{Sb}_x)_2\text{Te}_3$ materials changed from p-type to n-type for a Bi percentage of about 5%, the n-type being observed for Bi percentages below 5%. An one hour annealing at 250°C was realized on the $(\text{Bi}_{1-x}\text{Sb}_x)_2\text{Te}_3$ films. The results showed that the Seebeck coefficient was positive whatever the composition, which is characteristic of p-type materials. A maximal Seebeck coefficient was observed for Bi atomic percentages varying from 6 to 14% with a value of about 170 μ V/K.

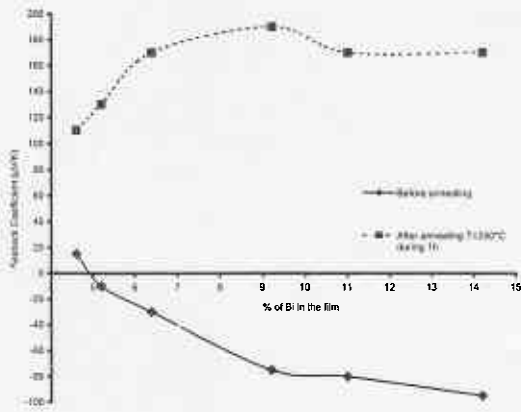


Fig.8 Evolution of the Seebeck coefficient with the Bi atomic percentage in the film ($E_{\text{deposition}}=-170$ mV/SCE, $[\text{Bi}^{\text{III}+}]+[\text{Sb}^{\text{III}+}]=[\text{Te}^{\text{IV}+}]=10^{-2}\text{M}$)

Figure 9 shows the evolution of the electrical resistivity ρ with the composition. Films having an important Sb atomic percentage present a strong resistivity in the order of $35000 \mu\Omega\cdot\text{m}$. When the Sb atomic percentage decreases, the electrical resistivity decreases too. After annealing, ρ decreases strongly under $1000 \mu\Omega\cdot\text{m}$. A minimal electrical resistivity is observed for Bi atomic percentages varying from 6 to 11% with a value of about $550 \mu\Omega\cdot\text{m}$.

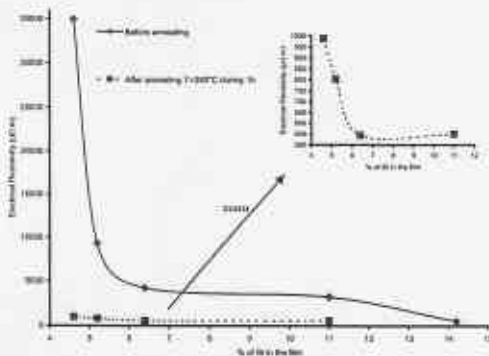


Fig.9 Evolution of the electrical resistivity with the Bi atomic percentage in the film ($E_{\text{deposition}}=-170$ mV/SCE, $[\text{Bi}^{\text{III}+}]+[\text{Sb}^{\text{III}+}]=[\text{Te}^{\text{IV}+}]=10^{-2}\text{M}$)

2. Pulse deposition

$(\text{Bi}_{1-x}\text{Sb}_x)_2\text{Te}_3$ films obtained by potentiostatic electrodeposition present an important roughness. In order to optimize the material morphologies, the synthesis pulse by current electrodeposition was studied. Indeed, this technique induces a higher rate of grain nucleation and results in a more refined grain structure, which benefits the deposit properties [23]. The next results are relating to the synthesis of $(\text{Bi}_{1-x}\text{Sb}_x)_2\text{Te}_3$ by pulse current deposition and to the influence of this technique on their thermoelectric and electrical properties.

✓ Determination of deposition parameters

The pulsed deposition process allows to achieve a higher cathodic intensity (I_c) and to change the interface between a cathode and solution by independently changing the pulse

parameters, such as anodic intensity (I_a), time of the cathodic pulse (T_c) and time between pulse (T_b).

In a first stage, we kept the electrolyte which gives the $\text{Bi}_{0.5}\text{Sb}_{1.5}\text{Te}_3$ ternary expected, that is $([\text{Bi}]+[\text{Sb}])/[\text{Te}]=1$ and $[\text{Sb}]/[\text{Bi}]=3$. The influence of cathodic current I_c has been studied. The other pulse parameters were fixed at $T_c=3\text{s}$, $T_b=10\text{s}$ and $I_a=0\text{mA}$. Figure 10 shows the reduction intensity dependence of $\text{Bi}_x\text{Sb}_y\text{Te}_z$ stoichiometry. For -10 to -2 mA range, the curves show that electrodeposited materials present an excess of Bi and Te and a deficit of Sb, compared with the expected stoichiometry.

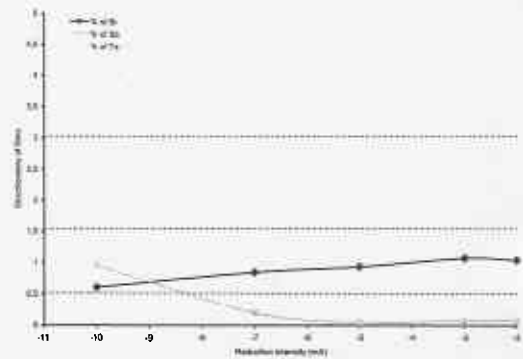


Fig.10 Reduction intensity of $\text{Bi}_x\text{Sb}_y\text{Te}_z$ stoichiometry $[\text{Bi}^{\text{III}+}]+[\text{Sb}^{\text{III}+}]=[\text{Te}^{\text{IV}+}]=10^{-2}\text{M}$, $[\text{Sb}^{\text{III}+}]/[\text{Bi}^{\text{III}+}]=3$, $T_c=3\text{s}$, $T_b=10\text{s}$, $I_a=0\text{mA}$

In order to get close to $\text{Bi}_{0.5}\text{Sb}_{1.5}\text{Te}_3$, the $[\text{Sb}]/[\text{Bi}]$ ratio was increased and was fixed at 6. As reduction intensity having given a film with a metallic aspect is about -5 mA, we studied the evolution of stoichiometry of films vs. the time of deposition with these parameters: $I_c=-5\text{mA}$, $T_b=5\text{s}$, $I_a=0\text{mA}$ (Figure 11).

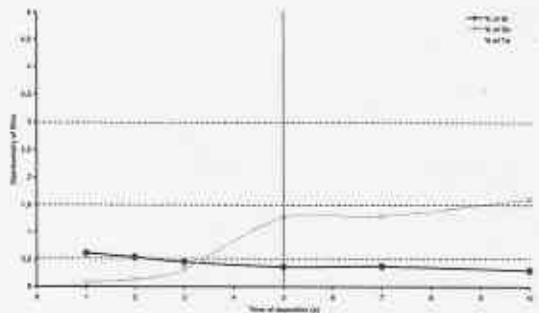


Fig.11 Time of deposition of $\text{Bi}_x\text{Sb}_y\text{Te}_z$ stoichiometry $[\text{Bi}^{\text{III}+}]+[\text{Sb}^{\text{III}+}]=[\text{Te}^{\text{IV}+}]=10^{-2}\text{M}$, $[\text{Sb}^{\text{III}+}]/[\text{Bi}^{\text{III}+}]=6$, $I_c=-5$ mA, $T_b=5\text{s}$, $I_a=0\text{mA}$

For short times of deposition ($T_c < 5\text{s}$), film stoichiometries present a high Te content and a very low Sb percentage. When T_c is superior to 5, the film stoichiometries obtained are closed to $\text{Bi}_{0.5}\text{Sb}_{1.5}\text{Te}_3$.

✓ Thermoelectric properties

The Seebeck coefficient and electrical resistivity measurements were performed on $(\text{Bi}_{1-x}\text{Sb}_x)_2\text{Te}_3$ materials in order to evaluate the influence of the pulse deposition vs. potentiostatic technique. These measurements were performed on films which compositions were $\text{Bi}_{0.36}\text{Sb}_{1.27}\text{Te}_{3.36}$.

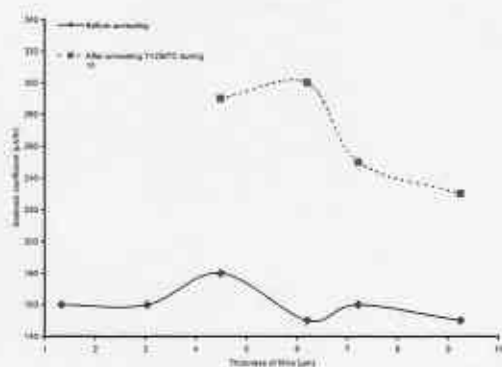


Fig.12 Evolution of the Seebeck coefficient with the thickness of films obtained by pulse electrodeposition ($[Sb^{III+}]/[Bi^{III+}]=6$, $I_c=-5$ mA, $T_c=5s$, $T_b=5s$, $I_a=0mA$)

The evolution of the Seebeck coefficient α with the thickness of films is reported in Figure 12. Values are positive and vary between 140 and 180 $\mu V/K$. After an one hour annealing at 250° the Seebeck coefficient strongly increased until the best value of 300 $\mu V/K$ for a thickness about 6 μm .

Figure 13 shows the evolution of the electrical resistivity ρ with the thickness of films. It appears that ρ increases with increasing thickness. After an one hour annealing at 250°C, films present a low electrical resistivity which do not exceed 100 $\mu\Omega.m$.

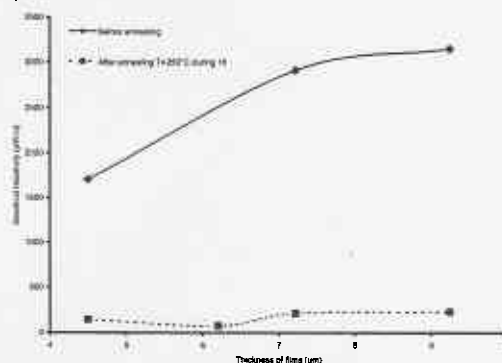


Fig.13 Evolution of the electrical resistivity with the thickness of films obtained by pulse electrodeposition ($[Sb^{III+}]/[Bi^{III+}]=6$, $I_c=-5$ mA, $T_c=5s$, $T_b=5s$, $I_a=0mA$)

Therefore, pulse electrodeposition allows to optimize the Seebeck coefficient and electrical resistivity, in particular after an one hour annealing at 250°C.

Conclusion

An electrolyte ($HClO_4$ 1M and $C_4H_6O_6$ 0,1M) has been used to electrodeposit Bi-Sb-Te ternary. The analytical studies and the position of the electrochemical ternary system have established the direct electroformation of alloys. By controlling the electrode potential or the electrolyte composition, it is possible to achieve a large range of ternary film compositions, in particular $Bi_{0,5}Sb_{1,5}Te_3$. The electrodeposited films of $(Bi_xSb_{1-x})_2Te_3$, corresponding to the solid solution, are polycrystalline. Thermoelectric and electrical properties can be improved using pulse electrodeposition techniques and annealing films at 250°C

during 1hour. A Seebeck coefficient equals to 300 $\mu V/K$ had been measured with a 6 μm thickness $Bi_{0,5}Sb_{1,5}Te_3$ film.

References

- [1] Nolas G.S. *and al*, Thermoelectrics: Basics Principles and New Materials Developments, Springer (2001)
- [2] Ohta T., Kajikawa T., Kumashiro Y., *Electr. Eng. Jpn.* Vol. 110, (1990) p.14
- [3] Kiely J.H., Lee D.H., *Meas. Sci. Technol.* Vol. 8 (1997) p.661
- [4] Hava S., Sequiera H.B., Hunsperger R.G., *J. Appl. Phys.* Vol. 58 (1985) p.1727
- [5] Lou D.Y., *Appl. Opt.* Vol. 21 (1982) p.1602
- [6] Ioffe A., Semiconductors Thermoelements and Thermoelectric Cooling, Infosearch, (London, 1957)
- [7] Yim B., Rosi F., *Solid State Electronics* Vol.15 (1957) p.1121
- [8] Ebisumori K., Tauchi H., Shinohara Y., Nishida I.A., *17th International Conference on Thermoelectrics* (1998) p.155
- [9] Seo J., Cho D., Park K., Lee C., *Materials research Bulletin* Vol. 35 (2000) p.2157
- [10] Koukharenko E., Frety N., Shepelevich V.G., Tedenac J.C., *J. Crystal Growth* Vol. 222 (2001) p.773
- [11] Kim H.C., Lee J.S., Oh T.S., Hyun D.B., Kolomoets N.V., *17th International Conference on Thermoelectrics* (1998) p.125
- [12] Zou H., Rowe D.M., Williams S.G.K., *Thin Solid Films* Vol. 408 (2002) p.270
- [13] Foucaran A., Sackda A., Giani A., Pascal-Delannoy F., Boyer A., *Mat. Sci. Eng.* B52 (1998) p.154
- [14] Damodara Das V., Gopal Ganesan P., *Solid State Com.* Vol. 106 (1998) p.315
- [15] Noro H., Sato K., Kagechika H., *J. Appl. Phys.* Vol. 73 (1993) p.1252
- [16] Takahashi M., Katou Y., Nagata K., Furuta S., *Thin Solid Films* Vol. 70 (1994) p.240
- [17] Magri P., Boulanger C., Lecuire J.M., *J. Mater. Chem.* Vol. 6 (1996) p.773
- [18] Miyazaki Y., Kajitani T., *J. Crystal Growth* Vol. 229 (2001) p.542
- [19] Fleurial J.P., Borshchevsky A., Ryan M.A., Philips W.M., Snyder J.G., Caillat T., Kolawa E.A., Herman J.A., Mueller P., Nicolet M., *Mater. Res. Soc.* Vol. 545 (1999) p.493
- [20] Michel S., Stein N., Schneider M., Boulanger C., Lecuire J.M., *J. Appl. Electrochem.* Vol. 33 No.1 (2003) p.23
- [21] Del Frari D., Diliberto S., Stein N., Boulanger C., Lecuire J.M., submitted in *Thin Solid Films* in July 2004
- [22] Villars P., Prince A., Okamoto H., Handbook of ternary alloy phase diagrams, Materials Park, OH ASM International (1995)
- [23] Puipe J.C., Leaman F., Theory and practice of pulse plating, (1986)